STANDARD ARTICLE

Journal of Veterinary Internal Medicine ACVIM

Open Access

American College of
Veterinary Internal Medicine

Long-term clinical and magnetic resonance imaging follow-up of dogs with osseous-associated cervical spondylomyelopathy

Carolyn Nye[1] | Eric Hostnik[1] | Elizabeth Parker[2] | Thomas Wittum[3] |
Stephen Jones[1] | Sarah Moore[1] | Laurie Cook[1] | Ronaldo C. da Costa[1]

[1]Department of Veterinary Clinical Sciences, The Ohio State University, Columbus, Ohio

[2]Department of Animal Sciences, The Ohio State University, Columbus, Ohio

[3]Department of Veterinary Preventative Medicine, The Ohio State University, Columbus, Ohio

Correspondence
Ronaldo C. da Costa, Department of Veterinary Clinical Sciences, The Ohio State University, 1010 Veterinary Medical Center, 601 Vernon Tharp Street, Columbus, OH 43210.
Email: dacosta.6@osu.edu

Funding information
Gray Lady Foundation

Abstract

Background: Osseous-associated cervical spondylomyelopathy (OA-CSM) is a complex disorder with limited long-term survival. The longitudinal progression is currently unknown.

Objective: To describe changes on magnetic resonance imaging (MRI) over a 2-year minimum period. We hypothesized that spinal lesions would progress in the majority of dogs.

Animals: Eleven dogs previously diagnosed with OA-CSM were prospectively studied. Nine dogs were treated medically, whereas 2 were treated surgically.

Methods: Clinical and MRI follow-up were performed with a median time between MRI studies of 30 months (range, 24-54). Morphologic assessment evaluated vertebral canal stenosis, spinal cord compression, foraminal stenosis, and articular processes, among other variables. Morphometric assessment included vertebral canal area, spinal cord area, area of the articular processes, and foraminal height.

Results: On follow-up MRI, the most affected site at the initial examination in medically treated dogs had progressed in 4 of 9 dogs, improved in 4, and was unchanged in 3. Clinically, all dogs except 2 medically treated dogs were unchanged to improve at follow-up. Initially, 50 of 60 (83.3%) intervertebral spaces had vertebral canal stenosis, whereas in the follow-up MRI 82.3% did. Of the sites with stenosis, 45.7% were unchanged, 18.6% improved, and 38.9% worsened. Morphometry identified significant decreases in vertebral canal and spinal cord areas at C4-C5 through C6-C7, and significant progression of articular process irregularities at C3-C4 and C6-C7.

Conclusions and Clinical Importance: This long-term follow-up study of dogs with OA-CSM did not identify clinical or MRI progression of lesions in the majority of dogs.

KEYWORDS

articular facet, longitudinal study, myelopathy, natural history, spinal cord, wobbler syndrome

1 | INTRODUCTION

Cervical spondylomyelopathy (CSM) is a common cause of neurologic deficits and pain in large and giant breed dogs.[1] Although no prevalence study exists, it often is considered the most common disease of the cervical spine in these dogs. Currently, a lack of consensus exists among veterinary neurologists regarding the best approach for treating CSM. This lack of consensus likely reflects limited understanding of the underlying disease mechanisms and natural progression, as well as the fact that CSM represents a collection of different etiologies and presentations rather than a single uniform disease.

Two documented forms of CSM exist: osseous-associated (OA-CSM), mainly seen in Great Danes and other giant breeds, and disc-associated (DA-CSM), seen in Doberman Pinschers and other large breed dogs. In both forms, abnormalities of the cervical vertebral column develop and result in static and dynamic spinal cord compression. In OA-CSM, compression results from osseous proliferation of the vertebral arch, articular processes, pedicles, or some combination of these.[1-3] Disc-associated cervical spondylomyelopathy results in compression secondary to intervertebral disc protrusion, often in combination with hypertrophy of the ligamentum flavum.[1,4] It generally is accepted that magnetic resonance imaging (MRI) is the imaging modality of choice for diagnosis and treatment planning in dogs with suspected CSM[1,5,6], but computed tomography (CT) can be particularly useful to document bony changes in dogs with OA-CSM.[7,8] The morphology and morphometry of the cervical spine in Great Danes with OA-CSM and Dobermans with DA-CSM, using MRI, have been reported previously.[2,7,9,10]

Cervical spondylomyelopathy may represent a naturally occurring canine clinical model of cervical spondylotic myelopathy, a degenerative syndrome of the cervical spine in people.[11] Cervical spondylomyelopathy in humans represents a complex syndrome consisting of variable degrees of degenerative change in the cervical vertebrae, intervertebral discs, facets and ligaments, which typically results in progressive myelopathy and radiculopathy.[12-18] The diagnosis of cervical spondylotic myelopathy in people is made using MRI to identify changes in the vertebral canal and spinal cord.[19] Some studies suggest dual imaging with computed tomography (CT) and MRI, using MRI for clarity of soft tissue details and CT to determine the extent of bony involvement,[20] but MRI remains the standard imaging modality for people with the condition.[19]

The natural progression of cervical spondylotic myelopathy in humans is described using clinical and long-term imaging follow-up studies, which are critical to understanding the disease and identifying factors associated with clinical deterioration.[21-25] Notably, a subset of people with MRI-documented CSM remain asymptomatic.[26] Few longitudinal studies have described the progression of structural changes in dogs with MRI-diagnosed CSM. A single longitudinal study was performed using MRI in dogs with DA-CSM,[11] whereas 2 others detailed findings in OA-CSM using CT for evaluation.[8,27] Therefore, our aim was to evaluate long-term changes in the vertebral canal and spinal cord using MRI in dogs treated medically and surgically for OA-CSM. We hypothesized that the majority of dogs would show progression of the vertebral and spinal cord lesions over the study period.

2 | MATERIALS AND METHODS

2.1 | Case selection

The study was reviewed and approved by the Ohio State University institutional animal care and use committee (IACUC; 2011A00 000027-R2) and written consent was obtained from all owners before enrollment. Medical and radiology records from January 2012 to June 2019 were searched for CSM cases using several terms to describe the disease. Dogs were included if they had a diagnosis of OA-CSM made by MRI a minimum of 2 years before study commencement. Exclusion criteria were diagnosis of DA-CSM as the predominant form of disease, follow-up time <24 months, or presence of comorbidities making anesthesia unsafe. Owners were contacted if there was a reasonable expectation of the dog still being alive and were asked whether they would be willing to enroll their dogs in a prospective study evaluating longitudinal MRI changes in OA-CSM.

All dogs had physical and neurologic evaluations, a CBC and serum biochemistry profile at both MRI time points.

2.2 | Neurologic grading

Neurologic status at the time of initial MRI and study enrollment was graded from 0 to 5, consistent with a previously published grading scale widely used in CSM studies:[11,27-29] grade 0, normal neurologic examination; grade 1, cervical hyperesthesia; grade 2, mild pelvic limb ataxia or paresis with or without thoracic limb involvement; grade 3, moderate pelvic limb ataxia or paresis with thoracic limb involvement; grade 4, marked pelvic limb ataxia or paresis with thoracic limb involvement; and grade 5, nonambulatory tetraparesis. Grading was performed using a combination of video recording and retrospective assignment based on neurologic examination forms.

2.3 | Initial magnetic resonance imaging

Initial MRI were identified and reviewed. Imaging was performed using a high-field MRI for all cases. In 10 dogs, a 3-Tesla (T) magnet (3.0 Tesla Achieva, Philips, Amsterdam, Holland) was used, whereas 1 dog had MRI using a 1.5 T magnet (1.5 T General Electric Signa, Milwaukee, Wisconsin). Dogs were placed in either dorsal or lateral recumbency.

2.4 | Follow-up magnetic resonance imaging

Follow-up MRIs were prospectively performed using the 3-Tesla magnet for all dogs. Anesthetic protocols were individually tailored based on clinical condition and clinician preference.

The MRI protocol included at a minimum T1- and T2-weighted images (WI) on all dogs in sagittal and transverse planes for intervertebral disc regions C4-5 to C6-7. Transverse images through the

disc spaces of C2-C3 to C7-T1 were available for review in 7 of the original MRIs and in 9 of the follow-up MRI. Neutral cervical spine positioning was used in both MRIs.

2.5 | Clinical case management

After initial MRI evaluation, 2 dogs were treated by dorsal laminectomy (1 at a single site and 1 at 2 sites) and 9 were treated medically using anti-inflammatory drugs and activity modification, both initial and long-term lifestyle changes. Lifestyle changes included minimizing high-impact activities such as running and jumping, rough play with other dogs, and off-leash strenuous activities. Walking wearing a body harness was encouraged. Individual treatment recommendations were made for each dog by the attending clinician using imaging findings, neurologic status, and the owner's preference.

2.6 | Morphologic evaluation

For morphologic analysis, MRI images were independently reviewed by 3 observers: a board-certified neurologist, a board-certified radiologist and a senior neurology resident (RdC, ETH, and CN) using 1 of 2 imaging software options: ClearCanvas Workstation (Clear canvas workstation, Synaptive Medical, Toronto, Ontario) or E-film (E-film workstation, IBM Watson Health, Armonk, New York). One of the observers (ETH) was blinded to the clinical status of the dogs. Vertebral canal stenosis and spinal cord compression were evaluated at each intervertebral disc region on T2-weighted transverse images as previously described.[7,9,30] Vertebral canal stenosis was graded as: 0, no compression; 1, partial subarachnoid space compression with no spinal cord compression; 2, complete subarachnoid space compression with no spinal cord compression; or 3, spinal cord compression. Spinal cord compression was further evaluated on the percentage of compression compared to normal area as previously described:[7,31] 0, no compression; grade 1, <25%; 2, 25-50%; or 3, >50% compression. Synovial cyst formation also was evaluated on transverse T2 WI: grade 0, no cyst formation; 1, cyst formation with no spinal cord compression; or 2, cyst formation with spinal cord compression.[7] Intervertebral disc degeneration was evaluated on sagittal T2 WI: grade 0, uniform hyperintense signal; 1, partial degeneration (partial loss of hyperintense signal); or 2, complete degeneration (no hyperintensity noted).[7]

Signal changes of the spinal cord and ligamentum or other soft tissue hypertrophy were evaluated on sagittal and transverse T2 or T1 WI, as previously described.[7] Areas of spinal cord hyperintensity were compared on sagittal and transverse images to normal areas of the spinal cord adjacent to the hyperintensity, and graded as: (0) normal, (1) mild (small or heterogeneous area of hyperintensity), or (2) severe (well defined or large area of hyperintensity). Ligament or soft tissue hypertrophy were areas isointense to muscle noted between the lamina and spinal processes, and were graded as: 0, no hypertrophy; 1, hypertrophy with no spinal cord compression; or 2, hypertrophy with spinal cord compression.

The remaining factors were evaluated bilaterally on sagittal or transverse T1 WI or both. Severity of foraminal stenosis was graded as: 0, no stenosis; 1, <33% stenosis; 2, 33-66% stenosis; or 3, >66% stenosis, based on the height of the intervertebral foramina. Regularity of the cranial and caudal articular processes was graded: 0, normal articular process; 1, smooth articular surface with evidence of bone sclerosis; or 2, irregular surfaces with subchondral sclerosis.[6-8] On the initial MRIs, 60 disc spaces and 120 articular processes and foramina were available for review on transverse imaging, with 66 disc spaces available on sagittal imaging. On follow-up imaging, 63 disc spaces and 126 articular processes and foramina were evaluated on transverse imaging whereas 66 disc spaces were evaluated on sagittal imaging. Fifty-nine disc spaces with 118 articular processes (transverse imaging) and 66 disc spaces (sagittal imaging) were available for direct comparison between initial and follow-up MRIs.

After individual MRI evaluations, each reviewer graded the initial and follow-up MRIs side-by-side as, same (unchanged), better or worse for all morphologic variables in addition to spinal cord atrophy. Spinal cord atrophy was assessed as an increase in the subarachnoid space surrounding the spinal cord.

2.7 | Morphometric evaluation

Morphometric assessments were performed by 1 reviewer (CN) using ClearCanvas Workstation software. For each dog, measurements of the initial MRI were made first, and then using the follow-up MRI. Measurements acquired included the area of the vertebral canal, spinal cord, any synovial cysts and the caudal and cranial articular processes, as well as foraminal height.[2,8] The vertebral canal area-to-spinal cord ratio was calculated for each disc site. Measurements were obtained from C2-C3 through C7-T1 when available. All measurements were performed within each intervertebral space at the slice of greatest compression. Foraminal stenosis was assessed on transverse images at the middle of the foramen.[2] To assess intraobserver agreement, each measurement was performed 3 times by the same reviewer with at least 24 hours between measurements.

2.8 | Statistical analysis

Morphologic data was assessed for interobserver reliability using the Kappa2 module[32] in Stata (StataCorp. Stata Statistical Software: Release 16. StataCorp LLC., College Station, Texas, 2019) to calculate a weighted Conger's Kappa for ≥3.[33] Agreement was determined as almost perfect for a kappa value between 0.81 and 1.0, substantial agreement as 0.61-0.8, moderate as 0.41-0.6, fair as 0.21-0.4, slight as 0.01-0.2, and <0 as poor agreement.[33]

To determine the repeatability of each measurement of the morphometric data, intraclass correlation (ICC) was used.[34] This procedure normally is used for correlation of quantitative observations among different observers, but in this case was used to determine the correlation among 3 replicates of measurement by 1 observer, with

0 being no agreement and 1 being perfect agreement. Because ICC was high, means of each assessment were calculated and used for comparison of the initial to follow-up MRI. Because the assumption of normality was questionable given the small sample size, Friedman's statistic was calculated using the snp2 module in Stata.[35] Friedman's analysis of variance (ANOVA) is the nonparametric equivalent of a 1-way repeated measure ANOVA. A Friedman's P-value <.05 was considered significant.

3 | RESULTS

Fifty-three dogs were identified during initial medical record review. Of these, 21 were dead, 2 had moved to a different area and were not available, and 19 were lost to follow-up. Eleven dogs with OA-CSM (9 male castrated, 1 female spayed and 1 female intact), with a mean age of 25.2 months at initial diagnosis (median, 18 months; range, 12-90 months) were identified from the medical records at The Ohio State University and prospectively recruited. Breeds represented included Great Danes (n = 6), German Shepherd (n = 2) and 1 each of the following: Greater Swiss Mountain Dog, Caucasian Ovcharka Dog, and Mastiff. Mean weight was 53.6 kg (median, 48.2 kg; range, 28.6-110 kg). All initial MRIs were performed between December 2012 and August 2017. Follow-up MRIs were performed a mean of 33 months later (median, 30 months; range, 24-54 months). The onset of clinical signs before initial evaluation ranged from 2 weeks to >1.5 years (mean, 6.7 months; median, 2.5 months). Historically, onset of clinical signs was acute in 1 dog, chronic in 8, and chronic with acute worsening in 2. Of the 9 dogs treated medically, initial neurologic examination was classified as grade 2 in 5 dogs, grade 3 in 3 dogs, and grade 4 in 1 dog. Six of these dogs were treated with PO prednisone (0.5 mg/kg q12, tapering progressively) and 1 with PO meloxicam (Meloxicam, Boehringer Ingelheim pharmaceuticals, Ingelheim am Rhein, Rhein, Germany; 0.1 mg/kg q24) after the initial MRI. At time of follow-up, 5 were still receiving corticosteroids, but the maintenance dose was low (eg, 0.2 mg/kg q48). Neurologically, at the time of follow-up examination, 5 were grade 2, 3 were grade 3, and 1 was grade 4. Of these, 2 dogs improved in neurologic grade (both from grade 3 to 2), 2 worsened (both from grade 2 to 3), and 5 remained unchanged. Of the 2 dogs treated surgically, 1 improved from grade 2 to grade 0, and the other remained unchanged at grade 2. Both dogs were still on PO prednisone at the time of follow-up examination.

Of the 9 dogs treated medically, the initial worst site of spinal cord compression improved in 2 dogs, worsened in 4 and remained the same in 3. Of the 2 that had improved spinal cord compression, 1 was clinically improved (grade 3 to 2) and the other showed no change in neurologic status. Of the 4 with worsening spinal cord compression, 1 had a worsened neurologic status (grade 2 to 3) whereas the others had not changed. Of the 2 dogs that underwent surgery, the extent of vertebral canal stenosis was graded better for all surgical sites, but the grade of stenosis did not change (grade 3). In the dog with 2 surgical sites (C3-4 and C4-5), the site immediately caudal to the surgical site (C5-C6) progressed from a grade 0 vertebral canal stenosis to grade 3. In the other dog that underwent surgery,

2 different sites cranial to the surgical site had worsened vertebral canal stenosis (grade 1 to 3 and grade 1 to 2). Of the 9 medically managed dogs, 4 sites of canal stenosis were worse (grade 1 to 3), with no more than 1 site per dog.

3.1 | Morphologic assessment

Regarding morphologic assessment, although interobserver agreement across all sites for vertebral canal stenosis was fair (kappa = 0.295) and for spinal cord compression was moderate (kappa = 0.511), perfect agreement was found among reviewers on determining the worst site of vertebral canal stenosis and spinal cord compression on initial MRI (kappa = 1). Additionally, there was agreement in 7/11 cases and majority agreement in 3/11 for evaluation of progression of disease at that site. Assessments were made by the most senior author (RdC) with extensive expertise and experience in evaluating MRI studies of dogs with CSM.

3.2 | Initial magnetic resonance imaging

All dogs had at least 1 site of vertebral canal stenosis, spinal cord compression, increased signal change in the spinal cord and articular process degeneration. Vertebral canal stenosis was present at 50/60 (83.3%) sites. The most common sites of vertebral canal stenosis were C2-C3 (7/7, 100%), C3-C4 (9/9, 100%), and C4-C5 (11/11, 100%). The next most common sites were C5-C6 and C6-C7 (10/11, 90.9% for both), and the least common was C7-T1 (3/9, 33.3%). Grade 3 vertebral canal stenosis resulting in spinal cord compression was identified in at least 1 site in all dogs and at 29/60 (48.3%) sites. The most common sites of grade 3 vertebral canal stenosis were C5-C6 and C6-C7 (8/60, 13.3% for both). Synovial cysts were identified in 2 dogs with 1 cyst per dog. The cysts were located at the articular processes of C3-C4 and C5-C6. Intervertebral disc degeneration was present in 8/11 dogs and appreciated at 26/66 (39.4%) sites. Grade 0 was present in 40/66 (60.6%), grade 1 in 23/66 (34.8%), and grade 2 in 3/66 (4.6%). The most common site was C6-C7, with 6/11 (54.6%). Signal change in the spinal cord was identified at 17/66 (25.8%) sites. Grade 0 was present in 49 (74.2%), grade 1 in 14 (21.2%), and grade 2 in 3 (4.6%). It was most common at C6-C7 (6/11, 54.6%) and least common at C7-T1 (0/11, 0%). Ligamentous hypertrophy was identified in 10/11 dogs and at 25/66 (37.9%) sites. Grade 0 was present in 41/66 sites (62.1%), grade 1 in 14/66 (21.2%), and grade 2 in 11/66 (16.7%). The most common site of ligamentous hypertrophy was C4-C5 (9/11, 81.8%), with the most common site resulting in compression of the spinal cord (grade 2) at C4-C5 (5/66, 7.6%). Intervertebral foraminal stenosis was present in 9/11 dogs and at 61/120 foramina (50.8%). Grade 0 was present in 59/120 (49.2%), grade 1 in 9/120 (7.5%), grade 2 in 24/120 (20%), and grade 3 in 28/120 (23.3%). The most common site was C5-C6 (17/22, 77.3%), and the least common site was C7-T1 (1/22, 4.6%). Irregularity of the articular process was identified in 101/118 (85.6%) articular processes, with grade 0 present in

17/118 (14.4%), grade 1 in 20/118 (17.0%), and grade 2 in 81/118 (68.6%). The most common site of irregularity was C5-C6 (22/22, 100%) followed by C4-C5 and C6-C7 (both 21/22, 95.4%).

3.3 | Follow-up magnetic resonance imaging

All dogs had at least 1 site of vertebral canal stenosis, spinal cord compression, increased signal change in the spinal cord and articular process degeneration. Vertebral canal stenosis was identified at 52/63 (82.5%) sites. The most common sites of vertebral canal stenosis were C2-C3 (8/8, 100%), C3-C4 (11/11, 100%), and C4-C5 (11/11, 100%). The next most common sites were C5-C6 and C6-C7 (10/11, 90.9% stenosis for both), and least common was C7-T1 (4/11, 36.4%). Vertebral canal stenosis resulting in spinal cord compression (grade 3) was identified at 30/63 (47.6%) sites. The most common site of grade 3 stenosis was C4-C5 (3/30, 10.0%). Synovial cysts were present in 4 dogs, with 2 cysts in 1 dog. Synovial cysts were present at C3-C4 and C4-C5 (2 at each) and 1 at C6-C7. Intervertebral disc degeneration was identified in 9/11 dogs and at 40/66 (60.6%) sites. Grade 0 was present in 26/66 (39.4%) sites, grade 1 in 31/66 (47.0%) and grade 2 at 9/66 (13.6%). The most common site was C6-C7 (9/11 dogs, 81.8%). Signal change in the spinal cord was identified in 9/11 dogs and at 19/66 (28.8%) sites. Grade 0 was present in 47 (71.2%) sites, grade 1 at 12 (18.2%), and grade 2 at 7 (10.6%). It was found equally at C3-C4, C4-C5, and C6-C7 (5/11 dogs, 45.5%). The least common site was C7-T1 (1/11, 9.1%). Ligamentous hypertrophy was identified in 10/11 dogs and at 40/66 (60.6%) sites. Grade 0 was present at 26/66 sites (39.4%), grade 1 at 31/66 (47.0%), and grade 2 at 9/66 (13.6%). The most common site was C4-C5 (10/11, 90.9%). Foraminal stenosis was present in 10/11 dogs and in 66 of 126 (52.4%) foramina. Grade 0 was present in 60/126 (47.6%), grade 1 in 13/126 (10.3%), grade 2 in 13/126 (10.3%), and grade 3 in 40/126 (31.8%). The most common site was C5-C6 (17/22, 77.3%). The second most common site was C4-C5 (16/22, 72.7%). The least common site was C7-T1 (5/22, 22.7%). Irregularity of an articular process was identified in 103/126 (81.8%) articular processes. Grade 0 was present in 23/126 (18.3%), grade 1 in 21/126 (16.7%), and grade 2 in 82/126 (65.1%). The most common site was C5-C6 (22/22, 100%) followed by C4-C5 and C6-C7 (20/22, 90.9% and 21/22, 95.5%, respectively).

3.4 | Comparison of initial and follow-up magnetic resonance imaging

Transverse images were available for comparison at 59 sites. Sixty-six sites were available for comparison on sagittal imaging. Of these, vertebral canal stenosis was unchanged in 25/59 (42.4%), improved in 11/59 (18.6%), and worsened in 23/59 (39.0%). The percentage of sites with vertebral canal stenosis remained relatively unchanged (50/60, 83.3% at initial time point; 52/63, 82.5% at follow-up). Spinal cord compression was unchanged in 30/59 (50.9%), improved in 12/59 (20.3%), and worsened in 17/59 (28.8%; Figure 1). The 2 initial synovial cysts
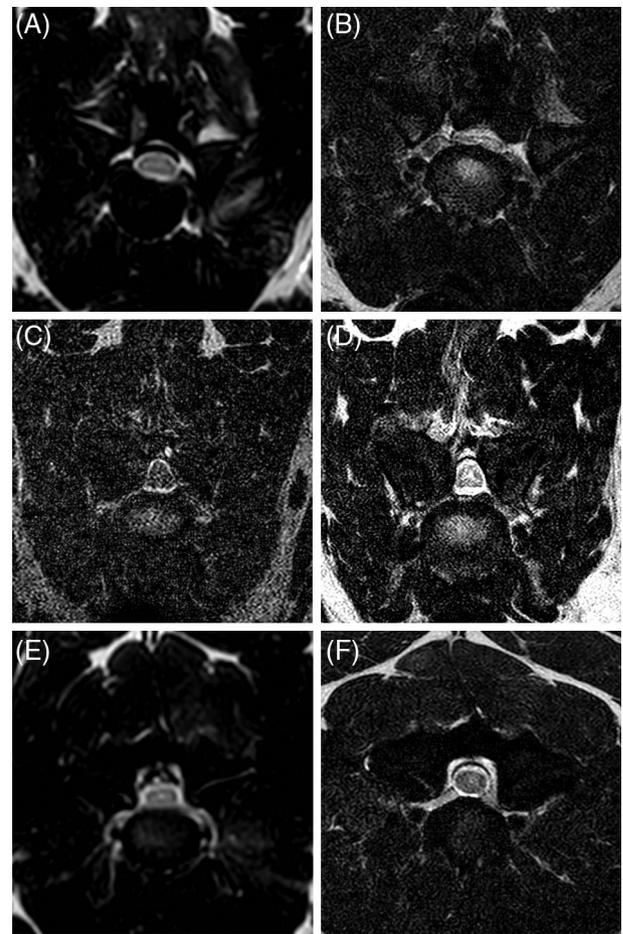

FIGURE 1　Magnetic resonance (MR) images of 3 dogs with osseous-associated cervical spondylomyelopathy. Left column shows the initial and right column shows the follow-up MR image. Each row shows images from the same dog at the same site. Figures A and B are from a 2-year-old female spayed Great Dane showing worsening of spinal cord compression at C5-6 over a 31 months follow-up period. Figures C and D are from a 1-year-old male castrated German shepherd dog showing minimal progression of spinal cord compression at C5-6 over a 24-month follow-up period. Figures E and F are from a 1-year-old, male castrated greater Swiss mountain dog showing improvement of spinal cord compression at C4-5 over a 29 month follow-up period

improved or resolved whereas 4 new cysts developed (Figure 2). Intervertebral disc degeneration was unchanged at 35/66 (53.0%), improved at 1/66 (1.5%), and worsened at 30/66 (45.5%) sites. In the 90/122 disc spaces on initial and follow-up MRI that showed grade 2 articular process irregularities, 42/90 (46.7%) also had disc degeneration. Similarly, of the 36/126 sites with grade 0 or 1 articular process irregularities, 17/36 (47.2%) had intervertebral disc degeneration. Signal changes within the spinal cord remained unchanged in 49/66 (74.2%), improved in 5/66 (7.6%), and worsened in 12/66 (18.2%). Of the 2 medically treated dogs that worsened clinically, both had increases in signal intensity at the worst site of vertebral canal stenosis, and 1 had a second site of increased signal intensity. Of the 2 medically treated dogs that improved clinically, 1 had improved signal intensity and the other had

worsened signal intensity. In the dogs that were clinically unchanged, signal intensity was unchanged in 1 dog and was worse in 4. Of the 2 dogs that clinically worsened, 1 had no change in signal intensity
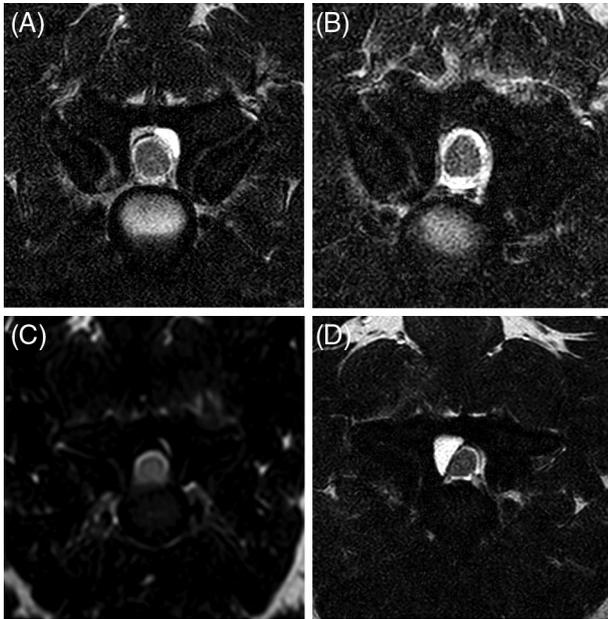

FIGURE 2 Magnetic resonance (MR) images of 2 dogs with osseous-associated cervical spondylomyelopathy. Left column shows the initial and right column shows the follow-up MR image. Figures A and B are from a 2-year-old Great Dane with improvement of a synovial cyst at C5-6 in the follow-up magnetic resonance imaging (MRI) at 30 months. Figures C and D are from a 2-year-old Great Dane showing development of a synovial cyst at C4-5 in the 24-month follow-up MRI

within the spinal cord, whereas the other had worsened. The 2 dogs treated surgically both had worsened signal change at the sites of surgery. Ligamentous hypertrophy was unchanged in 47/66 (71.2%), improved in 5/66 (7.6%), and worsened in 14/66 (21.2%). Foraminal stenosis was static in 102/120 (85.0%), improved in 3/120 (2.5%), and worsened in 15/120 (12.5%). Articular process irregularity was unchanged in 69/118 (58.5%), improved in 8/118 (6.8%), and worsened in 41/118 (34.7%). Spinal cord atrophy worsened at 15/65 sites (23.1%). The most common sites of worsened spinal cord atrophy were C5-C6 and C6-C7 (both 4/11; 36.4%).

3.5 | Morphometric analysis

The intraobserver reliability (ICC) for measurements for each location ranged from 0.279 to 0.997 (mean, 0.946; median, 0.977).

Vertebral canal area was significantly smaller at C4-C5, C5-C6, and C6-C7 on follow-up MRI measurements compared to initial MRI (P = .001, .001, .03, respectively). Spinal cord area also was significantly decreased at C4-C5, C5-C6, C6-C7, and C7-T1 on follow-up MRI (P = .04, .001, .03, .01, respectively). Left and right cranial articular processes were significantly larger at C2-C3 and C6-C7 but not at other sites (P = .02, .002, respectively). A full summary of significant differences is presented in Table 1. No statistical significance was found when comparing the initial MRI to follow-up MRI in the following categories: vertebral canal area at C2-C3, C3-C4, or C7-T1; spinal cord area at C2-C3 or C3-C4; vertebral canal-to-spinal cord area ratio from C2-3, C3-C4 and from C5-6 through C7-T1; synovial cyst area; foraminal height; caudal articular process proliferation; and, cranial articular process proliferation at C2-C3, C4-C5, C5-C6, and C7-T1.

TABLE 1 Significant findings on morphometric evaluation of initial and follow-up MRIs

Location and variable measured	Initial average	Follow-up average	% change	P-value for Friedman's ANOVA	Intraclass correlation
C3-C4 left cranial articular process	1.19 cm^2	1.43 cm^2	19.9	.02	0.98
C3-C4 right cranial articular process	1.18 cm^2	1.29 cm^2	8.6	.02	0.991
C4-C5 vertebral canal area	1.20 cm^2	0.85 cm^2	−30	.001	0.995
C4-C5 spinal cord area	0.41 cm^2	0.34 cm^2	−16	.03	0.897
C4-C5 vertebral canal : spinal cord	0.34	0.43	18	.001	0.948
C5-C6 vertebral canal area	1.14 cm^2	0.98 cm^2	−14	.001	0.993
C5-C6 spinal cord area	0.47 cm^2	0.35 cm^2	−26	.001	0.989
C6-C7 vertebral canal area	1.29 cm^2	1.1 cm^2	−14	.03	0.995
C6-C7 spinal cord area	0.50 cm^2	0.44 cm^2	−13	.03	0.961
C6-C7 left cranial articular process	1.28 cm^2	1.47 cm^2	15	.002	0.992
C6-C7 right cranial articular process	1.24 cm^2	1.47 cm^2	19	.002	0.985
C7-T1 spinal cord area	0.46 cm^2	0.38 cm^2	−17	.01	0.591

Notes: Demonstrating the location and variable measured that were significantly different between initial and follow-up MRI studies. Average of 3 values on morphometric assessment for the initial and follow-up studies, percentage change between the initial and follow-up measurements, the P-value for Friedman's ANOVA for the difference between initial and follow-up MRI averages, and the intraclass correlation to assess repeatability of each morphometric assessment.

Abbreviations: ANOVA, analysis of variance; MRI, magnetic resonance imaging.

4 | DISCUSSION

We documented the long-term evolution of clinical and vertebral changes in dogs with OA-CSM. To our knowledge, ours is the first study to document spinal changes in dogs evaluated by MRI ≥24 months after initial MRI. Morphologic assessment of the most affected site identified progression of disease in 4 of 9 dogs treated medically, improvement in 2, and no significant changes in 3. Vertebral canal stenosis improved at the surgical site in both dogs that underwent decompressive surgery. Clinical signs of OA-CSM were improved, unchanged or progressed slowly, with 9 dogs being unchanged or improved at follow-up, and none progressing >1 neurologic grade, regardless of changes observed on MRI or the treatment provided.

Morphologic assessment was paired with morphometric analysis to offer a more objective evaluation of progression of structure changes in the vertebral column and spinal cord. Significant differences were found in 5 variables assessed morphometrically between initial and follow-up MRI, which differs from a recent study that evaluated progression of OA-CSM using CT imaging, in which no significant differences were found.[8] Our results indicated progression of articular facet abnormalities, reduction of spinal cord area and reduction of vertebral canal area. Significant changes between initial and follow-up MRIs were identified at sites C3-C4 through C6-C7, with significant differences on >1 variable from C4-5 through C6-C7, consistent with previously reported common sites associated with CSM.[2,36-39] The increased prevalence of changes in the caudal cervical vertebral column compared to the cranial cervical region likely is reflective of increased movement of the vertebral column in this area.[40]

On morphometric examination, significant progression of vertebral canal stenosis was observed at C4-C5, C5-C6, and C6-C7 (3/6; 50% of the measured disc spaces). On morphologic assessment, 23/59 (39.0%) of sites of vertebral canal stenosis worsened. Similarly, there was a higher amount of change in spinal cord compression and resulting area of the spinal cord on morphometric analysis compared to morphologic analysis (4/6; 66.7% and 17/59; 28.8% change, respectively), but similar rates of perceived articular facet changes (2/6; 33.3% and 41/118; 34.7%).

Although in many instances there was agreement between the morphologic and morphometric assessments, the morphometric assessments demonstrated more differences. This disparity potentially reflects human error being involved more with morphologic assessment, which is supported by the variation in interobserver agreement despite having strict assessment criteria. Differences in morphologic and morphometric assessments were found in a CT study, in which differences were attributed to changes in positioning and relation of vertebra secondary to surgical changes.[27] Most of the significant changes on morphometric examination were in vertebral canal and spinal cord area, and most appeared concurrently. Changes in the spinal cord and vertebral column are likely more difficult to assess visually when occurring together, as often is the case with vertebral canal stenosis and spinal cord atrophy.[11] The decrease in both makes subtle changes more difficult to appreciate on morphologic assessment.

Importantly, although 1 explanation for the discrepancies is that morphometrics are more sensitive, a retrospective study assessing reviewer measurement across a variety of imaging modalities and anatomical structures cautioned readers about the unreliable nature and overinterpretation of morphometric values.[39]

Extradural synovial cysts arise from periarticular joint tissue and are seen in approximately 20% of dogs with OA-CSM.[40] In our study, 2 cysts seen on initial imaging resolved, whereas 4 new ones developed. For 1 of the cysts that resolved, the same dog developed 2 new cysts. It is unknown why the cysts resolved, but CSM is a dynamic process, and it is possible that cysts improve and worsen with different positioning of the vertebral canal.[41] A recent case report showed decreases in synovial cyst size over 3.5 years in the lumbosacral spine of a dog.[42] Proposed mechanisms for decreased cyst size included restoration of stability, spontaneous rupture, and use of anti-inflammatory drugs.[42] In the human medical literature 3 reports document resolution of synovial cysts.[43-45]

The clinical relevance of spinal cord signal changes seen on MRI is unclear.[46] In our study, medically managed dogs remained static clinically, but showed progression of spinal cord changes. Both dogs that had surgery had progression of spinal cord signal changes but remained either clinically static or improved. Signal changes within the spinal cord of dogs with CSM are significantly more likely in dogs with a chronic history, more severe neurologic deficits, and with moderate or severe spinal cord compression.[47]

Articular process changes are a key feature of OA-CSM and 1 of the most common causes of vertebral canal stenosis and spinal cord compression in dogs with this disease.[5-7] The caudal articular processes are shown to be 45% and 37% larger in dogs with CSM at C5-C6 and C6-C7, compared to breed-matched controls, and the cranial articular processes at C6-C7 are 26% larger.[2] In our study, significant progression of articular process proliferation was observed, showing that not only is there increased proliferation in dogs with CSM compared to those without, but also that it progresses. Although the exact pathophysiology causing these changes is unknown, studies in humans have demonstrated that osteoarthritic changes of the articular processes related to age result from adjacent disc degeneration[48-50] secondary to a combination of genetic predisposition, previous injury, obesity, abnormal biomechanics and joint overload.[48,50,51] This situation is different than that of the OA-CSM canine population, in which articular osteoarthritis tends to occur in young adult dogs because it is not always associated with intervertebral disc degeneration.[2]

Of the 2 dogs that underwent surgery, both had worsening of vertebral canal stenosis at 3 sites adjacent to the dorsal laminectomies, 2 of them resulting in spinal cord compression. In comparison, of the 9 medically managed dogs (53 disc sites assessed), only 4 additional sites of compression were identified. These findings are consistent with those of other studies describing the "domino effect," or adjacent segment disease, which is reported in up to 20% of dogs with CSM treated surgically[52] and is described as degeneration of intervertebral sites adjacent to sites with surgical correction. In a long-term follow-up study of OA-CSM dogs treated by surgical distraction and stabilization, 1 of 7 developed a "domino" lesion.[27] Some studies in DA-CSM dogs have

8 | Journal of Veterinary Internal Medicine

ACVIM
Open Access
American College of
Veterinary Internal Medicine

NYE ET AL.

shown that these adjacent segment lesions were more common with stabilization techniques as opposed to decompressive techniques,[53,54] whereas other studies showed no difference in patients undergoing surgery with or without stabilization techniques.[52]

Limitations of our study are the small number of cases examined as well as the small number that were surgically managed compared with medically managed dogs. Because long-term MRI follow-up is difficult to achieve, we included surgically and medically managed dogs to better understand not only the natural progression of the disease, but also the influence of surgery on nearby sites. Another limitation is that the MRI protocol was not standardized for all cases in the initial and follow-up studies, but all dogs were imaged using high-field MRI scanners and with an overall similar protocol. Although interobserver agreement was variable, for the variables with slight or worse agreement, many were falsely lowered because the expected agreement was close to 100%. Therefore, slight variations caused large changes to kappa, and agreement likely was better than portrayed statistically.

Long-term follow-up remains a pivotal feature for understanding the progression of lesions seen in OA-CSM. Previously 3 reports on long-term outcome of dogs with CSM have been published. Two of these were done using CT[8,27] and 1 using MRI evaluated DA-CSM in Doberman pinchers.[9] Ours is the first study to evaluate long-term changes using MRI in dogs with OA-CSM. Although the study on Dobermans identified very little progression over 1 year, our study identified more changes over the ≥2-year follow-up period. This result might be in part because of the passage of time, or differences in pathophysiology between OA-CSM and DA-CSM. Although our study showed that most dogs stabilize clinically, a subset of patients were still alive at least 2 years after initial diagnosis. The conclusions may not reflect the overall population of dogs with OA-CSM.

CONFLICT OF INTEREST DECLARATION

Authors declare no conflict of interest.

OFF-LABEL ANTIMICROBIAL DECLARATION

Authors declare no off-label use of antimicrobials.

INSTITUTIONAL ANIMAL CARE AND USE COMMITTEE (IACUC) OR OTHER APPROVAL DECLARATION

Approval from The Ohio State University IACUC (2011A00000027-R2).

HUMAN ETHICS APPROVAL DECLARATION

Authors declare human ethics approval was not needed for this study.

ORCID

Carolyn Nye https://orcid.org/0000-0003-3412-2260
Eric Hostnik https://orcid.org/0000-0002-7651-4775
Stephen Jones https://orcid.org/0000-0002-5515-8644
Sarah Moore https://orcid.org/0000-0002-4311-6199

REFERENCES

1. da Costa RC. Cervical spondylomyelopathy (wobblers syndrome) in dogs. *Vet Clin Small Anim Pract*. 2010;40:881-913.
2. Martin-Vaquero P, da Costa RC, Lima CGD. Cervical spondylomyelopathy in Great Danes: a magnetic resonance imaging morphometric study. *Vet J*. 2014;201(1):64-71.
3. Trotter EJ, De Lahunta A, Geary JC, Brasmer TH. Caudal cervical vertebral malformation-malarticulation in Great Danes and Doberman pinchers. *J Am Vet Med Assoc*. 1976;168:917-930.
4. Lewis DG. Cervical spondylomyelopathy ('wobbler' syndrome) in the dog: a study based on 224 cases. *J Small Anim Pract*. 1989;30:657-665.
5. Lipsitz D, Levitski RE, Chauvet AE, Berry WL. Magnetic resonance imaging features of cervical stenotic myelopathy in 21 dogs. *Vet Radiol Ultrasound*. 2001;42:20-27.
6. Gutierrez-Quintana R, Penderis J. MRI features of cervical articular process degenerative joint disease in Great Dane dogs with cervical spondylomyelopathy. *Vet Radiol Ultrasound*. 2012;53:304-311.
7. Martin-Vaquero P, da Costa RC, Drost WT. Comparison of noncontrast computed tomography and high-field magnetic resonance imaging in the evaluation of Great Danes with cervical spondylomyelopathy. *Vet Radiol Ultrasound*. 2014;55(5):496-505.
8. Vansteenkiste D, Martin-Vaquero P, Bonelli M, da Costa LB, da Costa RC. Long-term computed tomography follow-up in Great Danes with or without signs of osseous-associated cervical Spondylomyelopathy. *BMC Vet Res*. 2019;15:90.
9. Da Costa RC, Parent JM, Partlow G, et al. Morphologic and morphometric magnetic resonance imaging features of Doberman pinschers with and without clinical signs of cervical spondylomyelopathy. *Am J Vet Res*. 2006;67:1601-1612.
10. De Decker S, Gielen IMVL, Duchateau L, et al. Morphometric dimensions of the caudal cervical vertebral column in clinically normal Doberman pinschers, English foxhounds and Doberman pinschers with clinical signs of disk-associated cervical spondylomyelopathy. *Vet J*. 2012;191(1):52-57.
11. da Costa RC, Parent JM. One-year clinical and magnetic resonance imaging follow-up of Doberman pinschers with cervical spondylomyelopathy treated medically or surgically. *J Am Vet Med Assoc*. 2007;231(2):243-250.
12. Boden SD, McCowin PR, Davis DO, Dina TS, Mark AS, Wiesel S. Abnormal magnetic-resonance scans of the cervical spine in asymptomatic subjects. *J Bone Jt Surg*. 1990;72:1178-1184.
13. Fujiwara K, Yonenobu K, Hiroshima K, Ebara S, Yamashita K, Ono K. Morphometry of the cervical spinal cord and its relation to pathology in cases with compression myelopathy. *Spine*. 1998;13:1212-1216.
14. Herzog RJ, Wiens JJ, Dillingham MF, Sontag MJ. Normal cervical spine morphometry and cervical spinal stenosis in asymptomatic professional football players. Plain film radiography, multiplanar computed tomography, and magnetic resonance imaging. *Spine*. 1991;16:S178-S186.
15. Kato F, Yukawa Y, Suda K, Yamagata M, Ueta T. Normal morphology, age-related changes and abnormal findings of the cervical spine. Part II: Magnetic resonance imaging of over 1,200 asymptomatic subjects. *Eur Spine J*. 2012;21:1499-1507.
16. Okada Y, Ikata T, Katoh S, Yamada H. Morphologic analysis of the cervical spinal cord, dural tube, and spinal canal by magnetic resonance imaging in normal adults and patients with cervical spondylotic myelopathy. *Spine*. 1994;19:2331-2335.
17. Sherman JL, Nassaux PY, Citrin CM. Measurements of the normal cervical spinal cord on MR imaging. *Am J Neuroradiol*. 1990;11:369-372.
18. Tierney RT, Maldjian C, Mattacola CG, Straub SJ, Sitler MR. Cervical spine stenosis measures in normal subjects. *J Athl Train*. 2002;37:190-193.

19. Tetreault LA, Dettori JR, Wilson JR, et al. Systematic review of magnetic resonance imaging characteristics that affect treatment decision making and predict clinical outcome in patients with cervical spondylotic myelopathy. *Spine*. 2013;38:S89-S110.

20. Shafaie FF, Wippold FJ 2nd, Fado M, Pilgram TK, Riew KD. Comparison of computed tomography myelography and magnetic resonance imaging in the evaluation of cervical spondylotic myelopathy and radiculopathy. *Spine*. 1999;24(17):1781-1785.

21. Goto S, Mochizuki M, Watanabe T, et al. Long-term follow-up study of anterior surgery for cervical spondylotic myelopathy with special reference to the magnetic resonance imaging findings in 52 cases. *Clin Orthop Relat Res*. 1993;291:142-153.

22. Harada A, Mimatsu K. Postoperative changes in the spinal cord in cervical myelopathy demonstrated by magnetic resonance imaging. *Spine*. 1992;17:1275-1280.

23. Maigne JY, Deligne L. Computed tomographic follow-up study of 21 cases of nonoperatively treated cervical intervertebral soft disc herniation. *Spine*. 1994;19:189-191.

24. Matz PG, Anderson PA, Holly LT, et al. The natural history of cervical spondylotic myelopathy. *J Neurosurg Spine*. 2009;11(2):104-111.

25. Okamoto A, Shinomiya K, Furuya K, et al. Postoperative magnetic resonance imaging in patients with cervical myelopathy. *Spine*. 1991;16: S530-S533.

26. Kovalova I, Kerkovsky M, Kadanka Z, et al. Prevalence and imaging characteristics of nonmyelopathic and myelopathic spondylotic cervical cord compression. *Spine*. 2016;41(24):1908-1916.

27. Lewis M, Olby NJ, Sharp NJH, Early P. Long-term effect of cervical distraction and stabilization on neurological status and imaging findings in giant breed dogs with cervical stenotic myelopathy. *Vet Surg*. 2013;42(6):701-709.

28. Foss K, da Costa RC. Kinetic and kinematic follow-up gait analysis in Doberman pinschers with cervical spondylomyelopathy treated medically or surgically. *J Vet Intern Med*. 2018;32(3):1126-1132.

29. McKee WM, Butterworth SJ, Scott HW. Management of cervical spondylopathy-associated intervertebral, disc protrusions using metal washers in 78 dogs. *J Small Anim Pract*. 1999;40:465-472.

30. De Decker S, Gielen IMVL, Duchateu L, Van Soens I, Vabegems V, et al. Low-field magnetic resonance imaging findings of the caudal portion of the cervical region in clinically normal Doberman pinchers and foxhounds. *AJVR*. 2010;71:428-434.

31. Da Costa RC, Echandi RL, Beauchamp D. Computed tomography myelographic findings in dogs with cervical spondylomyelopathy. *Vet Radiol Ultrasound*. 2012;53:64-70.

32. Lazaro J, Zamora J, Abraira V, Zlotnik A. *KAPPA2: Stata module to produce Generalizations of weighted kappa for incomplete designs*. Boston, MA: Boston College Department of Economics; 2013.

33. Klein D. Assessing inter-rater agreement in Stata. *15th German Stata Users Group Meeting*. Berlin, Germany: University of Kassel; 2017.

34. *Intraclass correlation coefficients*. https://www.stata.com/features/overview/intraclass-correlation-coefficients/. Accessed March 1, 2020.

35. Goldstein R. Friedman's ANOVA test and Kendall's coefficient of concordance. snp2_1.pkgedn. *Stata Tech Bull*. 1992;1(3):1-28.

36. da Costa RC, Parent JM, Holmberg DL, Sinclair D, Monteith G. Outcome of medical and surgical treatment in dogs with cervical spondylomyelopathy: 104 cases (1988-2004). *JAVMA*. 2008;223(8): 1284-1290.

37. Provencher M, Habing A, Moore SA, et al. Kinematic magnetic resonance imaging for evaluation of disc-associated cervical Spondylomyelopathy in Doberman pinschers. *JVIM*. 2016;30:1121-1128.

38. Johnson JA, da Costa RC, Bhattacharya S, Goel V, Allen MJ. Kinematic motion patterns of the cranial and caudal canine cervical spine. *Vet Surg*. 2001;40:720-727.

39. Lamb CR, Nelson JR. Diagnostic accuracy of tests based on radiologic measurements of dogs and cats: a systematic review. *Vet Radiol Ultrasound*. 2014;56(3):231-244.

40. da Costa RC, Cook LB. Cystic abnormalities of the spinal cord and vertebral column. *Vet Clin Small Anim*. 2016;46:277-293.

41. Provencher M, Habing A, Moore SA, Cook L, Phillips G, da Costa RC. Evaluation of osseous-associated cervical spondylomyelopathy in dogs using kinematic magnetic resonance imaging. *Vet Radiol Ultrasound*. 2017;58:411-421.

42. Bonelli MA, da Costa RC. Spontaneous regression of extradural intraspinal cysts in a dog: a case report. *BMC Vet Res*. 2019;15:396.

43. Maezawa Y, Baba H, Uchida K, Furusawa N, Kubota C, Yoshizawa K. Spontaneous remission of a solitary intraspinal synovial cyst of the lumbar spine. *Eur Spine J*. 2000;9:85-88.

44. Mercader J, Gomez J, Cardenal C. Intraspinal synovial cyst: diagnosis by CT-follow-up and spontaneous remission. *Neuroradiology*. 1985; 27:346-348.

45. Swartz PG, Murtagh FR. Spontaneous resolution of an intraspinal cyst. *AJNR*. 2003;24:1261-1263.

46. Ohshio I, Hatayama A, Kaneda K, Takahara M, Nagashima K. Correlation between histopathologic features and magnetic resonance images of spinal cord lesions. *Spine*. 1993;18(9):1140-1149.

47. da Costa R. Relationship between spinal cord signal changes and clinical and MRI findings in dogs with cervical spondylomyelopathy – 102 cases. *J Vet Int Med*. 2012;26(3):807-808.

48. Gellhorn AC, Katz JN, Suri P. Osteoarthritis of the spine: the facet joints. *Nat Rev Rheumatol*. 2013;9:216-224.

49. Jaumard NN, Welch WC, Winkelstein BA. Spinal facet joint biomechanics and mechanotransduction in normal, injury and degenerative conditions. *J Biomech Eng*. 2011;133:071010.

50. Maus TP. Imaging of spinal stenosis: neurogenic intermittent claudication and cervical spondylotic myelopathy. *Radiol Clin North Am*. 2012;50:651-679.

51. Bogduk N. Degenerative joint disease of the spine. *Radiol Clin North Am*. 2012;50:613-628.

52. Jeffery ND, McKee WM. Surgery for disc-associated wobbler syndrome in the dog an examination of the controversy. *J Small Anim Pract*. 2001;42:574-581.

53. Rusbridge C, Wheeler SJ, Torrington AM, Pead MJ, Carmichael S. Comparison of two surgical techniques for the management of cervical spondylomyelopathy in Dobermans. *J Small Anim Pract*. 1998;39: 425-431.

54. Wilson ER, Aron DN, Roberts RE. Observation of a secondary compressive lesion after treatment of caudal cervical spondylomyelopathy in a dog. *J Am Vet Med Assoc*. 1995;2:153-154.